Development 129, 467-477 (2002)
Printed in Great Britain © The Company of Biologists Limited 2002
DEV3516

Brn3b/Brn3c double knockout mice reveal an unsuspected role for Brn3c in retinal ganglion cell axon outgrowth

Steven W. Wang[1], Xiuqian Mu[1], William J. Bowers[2], Dong-Seob Kim[3], Daniel J. Plas[3], Michael C. Crair[3], Howard J. Federoff[2], Lin Gan[2] and William H. Klein[1,*]

[1]Department of Biochemistry and Molecular Biology, The University of Texas M. D. Anderson Cancer Center, Houston, TX 77030, USA
[2]Center for Aging and Developmental Biology and Department of Neurology, University of Rochester School of Medicine, Rochester, NY 14642, USA
[3]Department of Neuroscience, Baylor College of Medicine, Houston, TX 77030, USA
*Author for correspondence (e-mail: wklein@mdanderson.org)

Accepted 22 October 2001

SUMMARY

In mice, Brn3 POU domain transcription factors play essential roles in the differentiation and survival of projection neurons within the retina, inner ear, dorsal root and trigeminal ganglia. During retinal ganglion cell differentiation, *Brn3b* is expressed first, followed by *Brn3a* and *Brn3c*. Targeted deletion of *Brn3b*, but not *Brn3a* or *Brn3c*, leads to a loss of most retinal ganglion cells before birth. However, as a few retinal ganglion cells are still present in *Brn3b*$^{-/-}$ mice, *Brn3a* and *Brn3c* may partially compensate for the loss of *Brn3b*. To examine the role of Brn3c in retinal ganglion cell development, we generated *Brn3b/Brn3c* double knockout mice and analyzed their retinas and optic chiasms. Retinal ganglion cell axons from double knockout mice were more severely affected than were those from *Brn3b*-deficient mice, indicating that Brn3c was required for retinal ganglion cell differentiation and could partially compensate for the loss of Brn3b. Moreover, Brn3c had functions in retinal ganglion cell differentiation separate from those of Brn3b. Ipsilateral and misrouted projections at the optic chiasm were overproduced in *Brn3b*$^{-/-}$ mice but missing were entirely in optic chiasms of *Brn3b/Brn3c* double knockout mice, suggesting that Brn3c controlled ipsilateral axon production. Forced expression of *Brn3c* in *Brn3b*$^{-/-}$ retinal explants restored neurite outgrowth, demonstrating that Brn3c could promote axon outgrowth in the absence of Brn3b. Our results reveal a complex genetic relationship between *Brn3b* and *Brn3c* in regulating the retinal ganglion cell axon outgrowth.

Key words: Brn3, POU domain transcription factors, Retina, Retinal ganglion cell differentiation, Axon outgrowth, Pathfinding, Mouse

INTRODUCTION

Projection neurons are typically defined as those that project long axons to different regions of neuronal or nonneuronal tissues. Examples include dorsal root ganglia, trigeminal ganglia and retinal ganglion cells (RGCs). Recent studies implicate the mouse Brn3 POU-domain transcription factors as key regulators for axon outgrowth and pathfinding in projection neurons (Huang et al., 1999; Gan et al., 1999; Wang et al., 2000; Erkman et al., 2000; Eng et al., 2001). Similarly, *Caenorhabditis elegans* UNC-86, an ortholog of the Brn3 factors, directly regulates the expression of genes involved in axonogenesis of mechanosensory neurons in the nematode (Sze et al., 1997; Duggan et al., 1998; Rohrig et al., 2000). In the mouse, Brn3 genes are expressed in projection neurons immediately after the cells exit mitosis and adopt specific neuronal fates. In addition, Brn3 genes are expressed postnatally (Xiang et al., 1995), suggesting a potential function in neuronal maintenance and survival in adult life. Further characterization of the Brn3 factors in mammalian neuronal development could thus shed light not only on de novo axon formation during embryogenesis but also on the failure of projection neurons to regenerate in adults (Goldberg and Barres, 2000).

In the mouse, the Brn3 family is composed of Brn3a, Brn3b and Brn3c (Pou4f1, Pou4f2 and Pou4f3, respectively – Mouse Genome Informatics). These factors share greater than 95% identity within their POU domains, suggesting that they have closely related functions in neuronal differentiation. The Brn3 genes are expressed in newly formed projection neurons with a high degree of spatial and temporal overlap. In the dorsal root ganglia, *Brn3a* expression is first observed at E9.5 (McEvilly et al., 1996). Expression of *Brn3b* and *Brn3c* follows that of *Brn3a*. In the developing retina, *Brn3b* expression is first detected at E11.5, when the first RGCs are formed. Expression of *Brn3a* begins 1 day later, followed by *Brn3c*, the last Brn3 gene expressed in the retina (Xiang et al., 1995; Gan et al., 1999). In cochlear and vestibular cells of the inner ear, *Brn3c* is the first of the Brn3 genes to be expressed, at approximately E14 (Xiang et al., 1997a) (S. W. W., unpublished). Thus, in

each sensory organ system, a different Brn3 gene is the first to be expressed.

Targeted deletions of the Brn3 genes affect the sensory systems in a manner that reflects the first gene that is expressed. Mice without *Brn3a* lose their suckling functions and show impaired somatosensory and motor control in large part because of abnormal trigeminal ganglia and dorsal root ganglia (McEvilly et al., 1996; Xiang et al., 1996a; Xiang et al., 1996b). By contrast, *Brn3b* knockout mice manifest a loss of a large number of RGCs (Gan et al., 1996; Erkman et al., 1996), and *Brn3c* knockout mice have hearing and vestibular defects because of cochlear and vestibular hair cell degeneration (Erkman et al., 1996; Xiang et al., 1997a). An interesting feature of the Brn3 knockout mice is that each displays a highly individualized phenotype that is not found in the others. Thus, no retinal or inner ear defects were associated with *Brn3a* knockout mice, no somatosensory/motor or inner ear defects were associated with *Brn3b* knockout mice and no somatosensory/motor or retinal defects were associated with *Brn3c* knockout mice.

The Brn3 factors are not required for the initial specification of sensory neurons but are essential for their normal differentiation and survival (Erkman, 1996; Xiang, 1998; Xiang et al., 1998; Gan et al., 1999; Wang et al., 2000; Eng et al., 2001). In *Brn3b* knockout mice, RGCs are specified and migrate to the ganglion cell layer, but most are not able to project normal axons, and eventually they undergo apoptosis (Xiang, 1998; Gan et al., 1999; Wang et al., 2000). Indeed, neuritic processes emanating from *Brn3b*-deficient RGCs assume a dendrite-like character indicating that Brn3b regulates the expression of genes critical for axon formation and may suppress dendrite formation. Whether Brn3a or Brn3c have a role in axonogenesis or other processes in RGCs remains unclear because in *Brn3a* and *Brn3c* knockout mice, Brn3b or other factors might compensate. A notable aspect of the *Brn3b*$^{-/-}$ phenotype is that 20% to 30% of the RGCs are able to send out axons, albeit abnormal ones, and these residual RGCs survive through adulthood (Wang et al., 2000; Erkman et al., 2001). These results predict that a more severe RGC phenotype might occur if one of the later expressed Brn3 genes was also deleted.

To test this prediction, we have generated *Brn3b/Brn3c* double knockout mice. Unlike *Brn3a*$^{-/-}$ mice, which die at birth, both *Brn3b*$^{-/-}$ and *Brn3c*$^{-/-}$ mice are viable and fertile. We expected that the *Brn3b/Brn3c* double knockout mice would also be viable. This expectation turned out to be true, and so we were able to characterize retinas and optic chiasms in postnatal double knockout animals. Our results show that Brn3c partially compensates for the loss of Brn3b because the double knockout mice had a greater loss of RGC axons than did the *Brn3b* knockout mice. Our experiments indicate that Brn3c plays an essential role in RGC axon formation. In addition, Brn3c appears to have distinct functions from those of Brn3b in axon pathfinding.

MATERIALS AND METHODS

Generation of *Brn3b/Brn3c* double knockout mice

We previously described a *Brn3b* knock-in allele in which *Brn3b* was replaced with the gene encoding human placental alkaline phosphatase (*AP*) (Gan et al., 1999). We also created *Brn3b-GFP* and *Brn3c-AP* alleles (L. G., unpublished). Mice deficient in both *Brn3b* and *Brn3c* were generated by mating *Brn3b* (*AP*/*AP*) or *Brn3b* (*GFP*/*GFP*) males with *Brn3c* (+/*AP*) females. All compound heterozygous animals appeared normal and were intercrossed to produce the *Brn3b* (*GFP*/*GFP*)*:Brn3c* (*AP*/*AP*) double knockouts that were used for subsequent experiments.

Semi-quantitative RT-PCR

Total RNA was isolated from retina of different embryonic stages by TriReagent (MRC), and first-strand cDNA was synthesized with Superscript reverse transcriptase (Life Technologies) at 42°C. cDNA equivalent equal to 40 ng of total RNA was used for PCR amplification with the Hotstart Taq DNA polymerase (Qiagen) in a volume of 20 μl. The reaction mixture was heated at 95°C for 15 minutes, denatured at 94°C for 30 seconds, annealed at 50°C for 30 seconds and extended at 72°C for 1 minute. Different cycle numbers were tested to determine the optimal cycle number for each reaction. The primers for PCR were as follows: *Brn3b*, forward, 5′-TCTGGAAGCCTACTTCGCCA-3′ and reverse, 5′-CCGGTT-CACAATCTCTCTGA-3′; *Brn3a*, forward, 5′-AGGCCTATTTTGC-CGTACAA-3′ and reverse, 5′-CGTCTCACACCCTCCTCAGT-3′; *Brn3c*, forward, 5′-TCTTCAACGGCAGTGAGCGT-3′ and reverse, 5′-ACACCCTGGAGTGTCCCGTA-3′; and *β-actin*, forward, 5′-CAACGGCTCCGGCATGTGC-3′ and reverse, 5′-CTCTTGCT-CTGGGCCTCG-3′. The PCR products were separated on a 2% agarose gel, and visualized using ethidium bromide.

Retinal tissue culture and AP staining

Retinal tissues were collected at E13.5 and dissected into four to eight pieces. Fresh retinal pieces were placed on laminin- (40 μg/ml) and poly-D-lysine- (100 μg/ml) coated coverslips in a six-well petri dish containing DMEM and 1% N2 neuronal supplement (Gibco BRL), 1% penicillin-streptomycin (Gibco BRL), and 0.2% glutamine (Gibco BRL). In addition to the DMEM, the final culture medium contained 5 μg/ml insulin, 100 μg/ml transferrin, 20 nM progesterone, 0.1 mM putrescine, 30 nM selenium, 100 U/ml penicillin, 100 μg/ml streptomycin, and 0.4 mM glutamine. Retinal explants were cultured for 2-3 days at 37°C with 5% CO_2 and air at 99% humidity.

Procedures for AP histochemical staining were modified from Fields-Berry et al. (Fields-Berry et al., 1992). Briefly, retinal explants were fixed with 3.2% paraformaldehyde (EMS) in 0.1 M phosphate-buffered saline (PBS) at pH 7.4 for 3 minutes. Fixed samples were rinsed four times with PBS for 10 minutes each and incubated at 65°C for 5 minutes to inactivate the endogenous AP activity. Heat-treated tissues were incubated in AP buffer (100 mM Tris-HCl (pH 9.5), 100 mM NaCl, 50 mM $MgCl_2$, and 2 mM levamisal (Sigma)) at room temperature for 30 minutes. Color reactions were carried out in AP detection solution (100 mg/ml BCIP (Sigma) and 1 mg/ml NBT (Sigma)) for 3 to 15 hours at room temperature. The samples were then post-fixed with 3.2% paraformaldehyde for 10 minutes at room temperature and washed twice with TE and once with PBS. Samples were mounted in Fluromount (EMS) for microscopy. Images were examined with an Olympus IX-70 inverted microscope and collected digitally.

Immunohistochemistry and confocal microscopy

Cryosections or wholemounts of retinal tissue were labeled with primary and secondary antibodies following standard immunohistochemical procedures. Briefly, fixed whole retinas or cryosections were washed three times with PBS containing 0.05% Triton X-100 (PBS-T) and blocked with 2% bovine serum albumin (BSA) in PBS-T for 1 hour. Samples were then incubated sequentially for 1 hour each with the first primary antibody, first secondary antibody, second primary antibody and second secondary antibody. Samples were washed three times with PBS-T between each antibody incubation. Primary antibodies were mouse anti-β3 tubulin

(Chemicon), rabbit anti-choline acetyltransferase (ChAT) (Chemicon) and mouse anti-neurofilament light chain (NFL) (Zymed). Secondary antibodies were Cy5-conjugated goat anti-rabbit IgG (Jackson ImmunoResearch Lab) and Alexa488-conjugated goat anti-mouse IgG (Molecular probes). Nuclei were visualized by quick rinsing in propidium iodide solution (1/3000 dilution of saturated solution). Labeled tissues were mounted in Fluoromount and examined using an Olympus FV500 confocal microscope equipped with argon, green HeNe and red HeNe lasers. Images were projected from 5 to 12 optical sections with intervals of 0.5 μm. Projected images were pseudo-colored to represent the colors as seen in an epifluorescence microscope. Cy5 emission was assigned blue.

Anterograde tracing of optic chiasms

Anesthetized P1 pups were used for anterograde tracing of RGC axons at the optic chiasm. DiI (Molecular Probes) and DiASP (Molecular Probes) were applied to different eyes using a Nanoject (Drummond). For each labeling, 70 nl of 10% DiI or DiASP dissolved in dimethyl formamide was injected three times at different spots of the ganglion cell layer within the tempo-ventral portion of the retina. Optic chiasms were collected from sacrificed mice 20 to 24 hours after injection. The collected optic chiasms were mounted on coverslips in Fluoromount for confocal microscopic analysis.

HSV amplicon vector construction and infection

The pHSVPrPUC/CMVegfp amplicon used in these experiments expresses the enhanced green fluorescence protein (eGFP) under the control of the CMV IE promoter and the gene of interest under control of the HSV IE4/5 promoter (Bowers et al., 2001). The pHSVBrn3c/CMVegfp amplicon was constructed by inserting a cDNA fragment encoding *Brn3c* into the *Xba*I and *Bam*HI sites of the parent amplicon. Helper virus-free amplicon packaging and virus purification were performed as described previously (Bowers et al., 2001). Viral infectivity was determined by assessing both GFP expression and transduction efficiency (Bowers et al., 2000). For infection, retinal tissues were incubated with 50 μl of viral products with the same volume of culturing media (Wang et al., 2000) at 37°C for 1 hour. Infected retinal tissues were then transferred to neural culture media with laminin-coated substrate (Wang et al., 2000).

RESULTS

Expression of *Brn3a* and *Brn3c* in retinas of *Brn3b*$^{-/-}$ embryos

To test whether *Brn3a* or *Brn3c* might partially compensate for the loss of Brn3b in RGC differentiation and survival, we first needed to determine whether *Brn3a* or *Brn3c* expression was affected in retinas of *Brn3b*$^{-/-}$ mice. In wild-type mice, *Brn3a* and *Brn3b* are expressed in almost all RGCs, while *Brn3c* is expressed in approximately 50% of the RGCs (Xiang et al., 1995; Gan et al., 1999). *Brn3a* and *Brn3c* expression is diminished in retinas of *Brn3b*$^{-/-}$ adults (Erkman et al., 1996; Gan et al., 1996), but the decreased expression is largely due to the presence of fewer RGCs (Gan et al., 1996).

To determine whether *Brn3a* and *Brn3c* were expressed in developing retinas of *Brn3b*$^{-/-}$ mice, we performed RT-PCR with RNA isolated from wild-type and *Brn3b*$^{-/-}$ E14.5 and E16.5 retinas. In the wild-type retinas, robust expression of *Brn3b* and *Brn3a* was observed at E14.5 and E16.5, while *Brn3c* expression was weak at E14.5 and increased several fold by E16.5 (Fig. 1). In *Brn3b*$^{-/-}$ retinas, *Brn3a* and *Brn3c* expression was attenuated to a half to a third of wild-type levels in both E14.5 and E16.5 retinas, but was nonetheless detectable (Fig. 1). Between E14.5 and E16.5, *Brn3b*$^{-/-}$ RGCs undergo enhanced apoptosis relative to controls (Xiang, 1998; Gan et al., 1999), and thus lowered expression levels for *Brn3a* and *Brn3c* were at least partially caused by the presence of fewer RGCs or RGCs undergoing programmed cell death. The RT-PCR experiments clearly indicated that although the absence of Brn3b attenuated *Brn3a* and *Brn3c* expression in the developing retina, expression was not abolished. The results are thus consistent with those of Gan et al. (Gan et al., 1996), who showed that expression of *Brn3a* and *Brn3c* in adult retinas was not noticeably altered on a per RGC basis. It therefore remained possible that *Brn3a* and *Brn3c* partially compensated for the loss of Brn3b in *Brn3b*$^{-/-}$ mice.

Defective axon outgrowth in RGCs of *Brn3b/Brn3c* double knockout mice

We chose to test whether *Brn3c* was required for RGC differentiation and whether it partially compensates for the loss of *Brn3b* by generating *Brn3b/Brn3c* double knockout mice. This choice was made because *Brn3b/Brn3c* double knockout mice, unlike *Brn3a-Brn3b* double knockout mice, were likely to be viable, which would allow us to examine retinal defects in adults as well as embryos. To facilitate the analysis, we inserted the *AP* gene into the *Brn3c* locus to create *Brn3c*-deficient mice (Fig. 2). The *Brn3b/Brn3c* double knockouts were deaf and had severe vestibular impairment (data not shown). The extreme vestibular defects were greater than those seen in *Brn3c* knockout mice, suggesting that *Brn3b*, in addition to *Brn3c*, might play a role in the differentiation of vestibular neurons within the inner ear. Despite their behavioral abnormalities, the *Brn3b/Brn3c* double knockouts survived to adulthood and were fertile.

It is known that *Brn3c* is expressed in approximately 50% of RGCs (Xiang et al., 1995). To determine whether *Brn3c* was required for axon outgrowth in this RGC subpopulation, we cultured retinal explants from *Brn3b*$^{+/+}$*:Brn3c* (*AP*/+) and *Brn3b*$^{+/+}$*:Brn3c* (*AP/AP*) embryos. If *Brn3c* was essential for axon outgrowth, *Brn3c*-expressing cells, which are defined as cells that would express *Brn3c* in wild-type retinas and are indicated by *AP* expression, should not be able to send out axons. We observed *AP* expression in axons emanating from

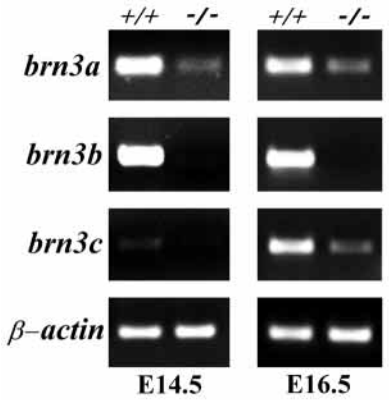

Fig. 1. Expression of *Brn3a*, *Brn3b* and *Brn3c* in developing retinas of wild-type and *Brn3b*$^{-/-}$ mice. *Brn3a*, *Brn3b*, *Brn3c* and *β-actin* transcripts were detected by RT-PCR. Total RNA was collected from wild-type (+/+) and *Brn3b*$^{-/-}$ retinas at E14.5 and E16.5. PCR products were visualized by ethidium bromide staining.

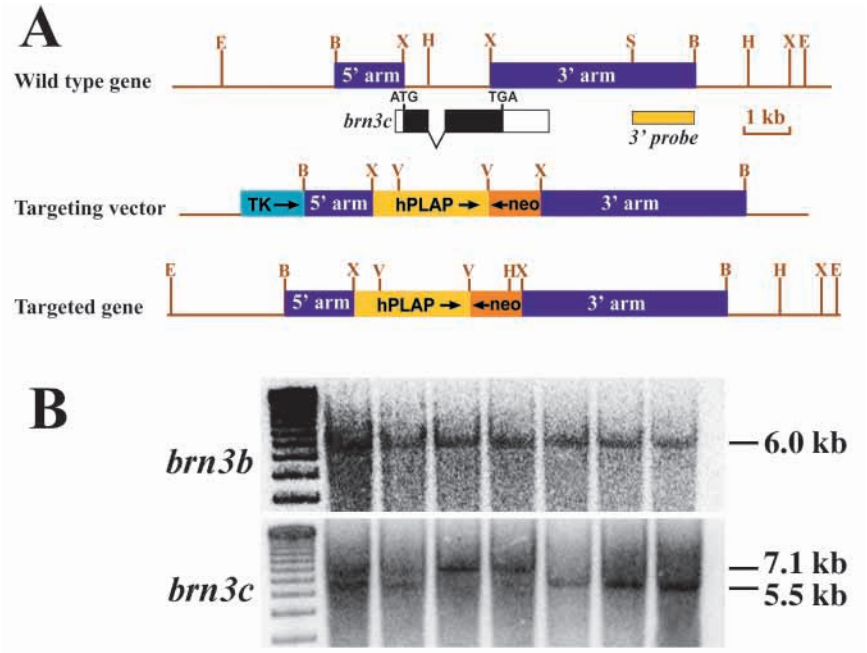

Fig. 2. Construction of the *Brn3c-AP* allele and genotype of *Brn3b/Brn3c* double knockout mice. (A) The 5′ and 3′ homology arms of *Brn3c* were inserted into the multiple cloning site of the *AP-ki* targeting vector (Gan et al., 1999). The targeting vector contains *TK*, *neo* and *AP* (*hPLAP*) cassettes as depicted. The position and exon/intron organization of the *Brn3c* gene with a 1.5 kb *Sac*1-*Bam*H1 fragment used for genotyping are shown below the wild-type gene. B, *Bam*HI; E, *Eco*RI; H, *Hin*dIII; S, *Sac*I; V, *Eco*RV; X, *Xba*I. (B) Genotypes from a *Brn3b*$^{-/-}$*:Brn3c* (+/–) intercross using Southern hybridization. Genomic DNA was digested with *Hin*dIII and *Bam*HI. Genotyping for *Brn3b* was performed as detailed by Gan et al. (Gan et al., 1999), and a band at 6-kb representing the targeted allele is observed in all lanes. Genotyping for *Brn3c* was performed using the 3′ probe shown in A, which resulted in a wild-type band (7.1 kb) and a mutant band (5.5 kb). The three right hand lanes represent genotypes of *Brn3b/Brn3c* double mutant mice.

Brn3c-expressing cells in both *Brn3c* heterozygous and homozygous null retinas (Fig. 3A-D). Thus, Brn3c was not required for axon outgrowth in *Brn3c*-expressing cells, at least not if Brn3b was present. *AP* expression was stronger in the *Brn3c* (*AP/AP*) explants than in *Brn3c* (*AP/+*) explants because there were two copies of *AP* rather than one (Fig. 3A,B).

We next determined whether axon outgrowth occurred in *Brn3c*-expressing cells in the absence of *Brn3b*. As expected from previous work (Wang et al., 2000), explants that marked *Brn3b*-expressing cells from *Brn3b* (*AP/AP*)*:Brn3c*$^{+/+}$ retinas displayed abnormal neurite outgrowth, suggestive of dendrites rather than axons (Fig. 3E). When *Brn3c*-expressing cells were identified by *AP* expression in a *Brn3b* (*GFP/GFP*)*;Brn3c* (*AP/+*) retinal explant, we also observed neurite outgrowth (Fig. 3G, arrows). By contrast, *Brn3c*-expressing cells from *Brn3b/Brn3c* double mutant explants were unable to send out any processes (Fig. 3F,H). The area of growing neurites of an explant from a *Brn3b* (*GFP/GFP*)*:Brn3c* (*AP/AP*) retina is shown in Fig. 3F and the tissue itself is shown in Fig. 3H. The cells from which the neurites grew did not express *AP* and so were not *Brn3c*-expressing cells (Fig. 3F, arrows). These cells were generating neurites independently of both Brn3b and Brn3c, perhaps through events controlled by Brn3a. Nevertheless, numerous viable cells that normally express *Brn3c* were present within the explanted tissue (Fig. 3H, arrowheads). We also observed fractured membrane debris marked by *AP* expression in the *Brn3b* (*GFP/GFP*)*;Brn3c* (*AP/AP*) retinal tissue indicating extensive apoptosis of *Brn3c*-expressing cells (Fig. 3H). Apoptosis may be the result of *Brn3c*-expressing cells not being able to project axons. It is also possible that some RGCs that lack both Brn3b and Brn3c factors were undergoing apoptosis within the explants before axonogenesis could occur. However, other RGCs lacking Brn3b and Brn3c did not appear apoptotic and yet were still not able to extend axons (Fig. 3H, arrowheads). It is likely that RGCs lacking Brn3b and Brn3c were abnormal both in their ability to survive and their ability to extend axons.

The results with cultured retinal explants demonstrate that *Brn3c* is not essential for axon outgrowth as long as *Brn3b* is present. However, in the absence of both *Brn3b* and *Brn3c*, *Brn3c*-expressing cells (as marked by *AP* expression from the *Brn3c* locus), are present but are unable to extend axons and undergo programmed cell death.

Elimination of optic fibers but not RGCs in E16.5 retinas of *Brn3b/Brn3c* double knockout mice

The experiments using retinal explants indicated that Brn3c had a role in RGC differentiation as a regulator of axon outgrowth and that it might partially compensate for the absence of Brn3b. If true, fewer optic fibers (RGC axons) should be detected in developing retinas that were deficient in both *Brn3b* and *Brn3c*. To examine this possibility, we monitored retinas from *Brn3b*$^{-/-}$ and *Brn3b/Brn3c* double knockout embryos for the expression of markers designed to visualize optic fibers and RGC nuclei. In wild-type E16.5 retinas, numerous axons coalesced counter-radially into the optic disk in a well-fasciculated fashion (Fig. 4A,B). Retinas that lacked only *Brn3c* appeared identical to wild-type retinas (data not shown). In *Brn3b*-deficient retinas, far fewer optic fibers were observed (Fig. 4D,E), consistent with earlier reports (Erkman et al., 1996; Gan et al., 1996). Moreover, the axons of *Brn3b*-deficient RGCs were not fasciculated and were misguided (compare Fig. 4B with 4E). They were entangled and crossed or by-passed the optic disk, growing toward the opposite side of the retina rather than entering the optic disk (Fig. 4E).

In *Brn3b/Brn3c* double mutant retinas, axons were difficult to detect at low magnification (Fig. 4G). Higher magnification revealed sparsely distributed axons (Fig. 4H). However, the few axons that were observed appeared to be correctly routed, unlike the misguided axons in *Brn3b*-deficient retinas (Fig. 4E,H). Despite the drastic decrease in axons, the overall cell number within the ganglion cell layer was not significantly different between *Brn3b*$^{-/-}$ and *Brn3b*$^{-/-}$*:Brn3c*$^{-/-}$ retinas (Fig.

4C,F,I). Thus, as was observed in vitro with explanted retinas, the loss of both *Brn3b* and *Brn3c* blocked axon outgrowth in the subpopulation of RGCs that would normally express both *Brn3b/Brn3c*. These results provided strong evidence for Brn3c functioning in RGC differentiation to promote axon outgrowth.

RGCs in adult retinas of *Brn3b/Brn3c* double knockout mice

The greater loss of axons in embryonic retinas of *Brn3b/Brn3c* double knockout mice suggested that adult retinas would also be affected. As is the case for *Brn3b*-deficient mice, we would expect RGCs that were unable to extend axons would not survive into postnatal life. Retinas were collected from 3-week-old mice and monitored for the expression of markers for RGCs and their axons, amacrine cells and cell nuclei (Fig. 5).

In the adult retinas, we found that different regions of retinas from double knockout mice were differentially affected. Within the dorsal-nasal region, *Brn3b/Brn3c* mutant retinas had only slightly fewer RGC axons than retinas from *Brn3b*$^{-/-}$ mice, although, as expected, neither genotype reached the number in wild type (Fig. 5A-C). However, within the ventral-temporal region, *Brn3b/Brn3c* double knockout retinas had far fewer axons than their *Brn3b*-deficient littermates (Fig. 5D-F, arrows indicate nonspecifically labeled blood vessels).

Cell numbers within the ganglion cell layer of the ventral-temporal region were also altered (Fig. 5G-I). Retinas lacking *Brn3b* had approximately 85% of the cells present in wild-type controls, whereas retinas of the double mutants had only 70% of the cells. However, the reduction in number was less than expected given the substantial loss of axons and was not reflective of the reported value for *Brn3b*$^{-/-}$ RGC loss (Gan et al., 1996). The discrepancy was explained by the replacement of RGCs with displaced amacrine cells, as revealed by ChAT staining of starburst amacrine cells (Fig. 5J-O).

Nuclei stained with propidium iodide showed two populations of cells within the ganglion cell layer, based on their size and intensity of staining (green and blue arrows in Fig. 5G-I). Those with large nuclei and diffuse propidium iodide staining were mostly RGCs, and those with small nuclei and intense staining were mostly starburst amacrine cells. In wild-type retinas, RGCs occupied most of the space in the ganglion cell layer with a few displaced amacrine cells scattered among them (Fig. 5G, Fig. 6). In *Brn3b*$^{-/-}$ retinas, there was a 65% reduction in the number of RGCs, while the number of displaced amacrine cells increased threefold (Fig. 5H, Fig. 6). In *Brn3b/Brn3c* double mutant retinas, the number of RGCs was reduced by 60% compared with that of *Brn3b*$^{-/-}$ retinas (Fig. 5I, Fig. 6).

In *Brn3b/Brn3c* mutant mice, it appeared that the loss of RGCs led to an increased percentage of cells in the ganglion layer that were displaced amacrine cells. To further substantiate this point, we prepared retinal sections at randomly selected orientations across the optic disk of *Brn3b*$^{-/-}$ and *Brn3b/Brn3c* double knockout mice at 3 weeks of age. As expected, the optic fiber (RGC axons) was substantially reduced in the *Brn3b*$^{-/-}$

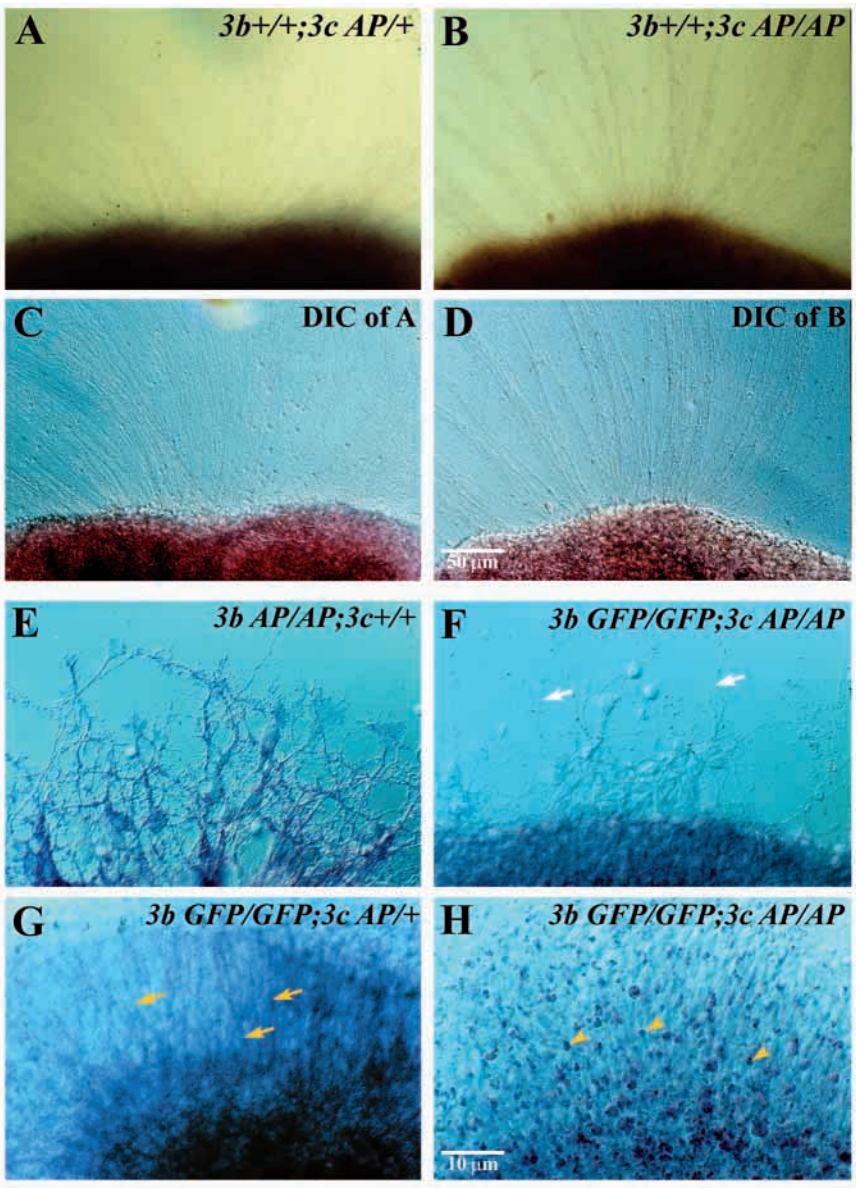

Fig. 3. Axons projecting from *Brn3c*-expressing cells in retinal explants. (A) Weak AP activity detected in axons projecting from a *Brn3c* (*AP/+*) retinal explant. (B) *AP* activity was twice as intense as in A in axons projecting from a *Brn3c* (*AP/AP*) retinal explant. (C,D) DIC images of A and B, respectively, showing abundant axons emanating from both of the retinal explants. (E) *AP* expression in neurites and migrating cells from a *Brn3b* (*AP/AP*) retinal explant. (F) Lack of *AP* expression in neurites and migrating cells from a *Brn3b* (*GFP/GFP*)*:Brn3c* (*AP/AP*) double mutant retinal explant. Arrows point to nonexpressing neurites. (G) *AP* expression in neurites (arrows) within the tissue body of *Brn3b* (*GFP/GFP*)*:Brn3c* (*AP/+*) retinal explants. (H) *AP* expression in *Brn3c*-expressing cells (arrowheads) within the tissue body of a *Brn3b* (*GFP/GFP*)*:Brn3c* (*AP/AP*) double mutant retinal explant.

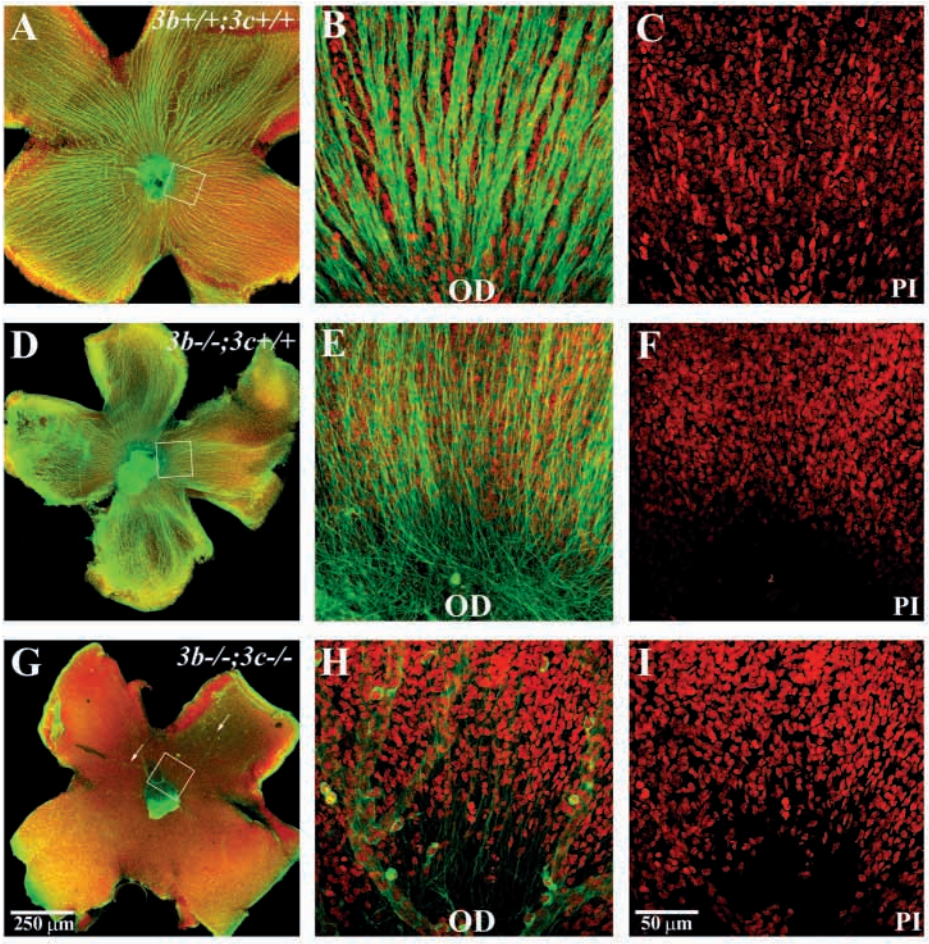

Fig. 4. Retinal flat-mounts showing RGCs and optic fiber layers from E16.5 retinas. (A) Low magnification of a wild-type retina labeled with anti-NFL (axons, green) and propidium iodide (nuclei, red). Axons were well fasciculated and were growing counter-radially into the optic disk (OD). (B) An enlarged view of the retina from the area highlighted in A. (C) Same image as B with the green channel (axons) removed. Note numerous nuclei in the ganglion cell layer. (D) Low magnification of *Brn3b*$^{-/-}$ retina labeled with the same antibodies as in A. (E) An enlarged view of the retina from the area highlighted in D. The axon number was greatly reduced when compared with that of a wild-type retina. Axons were not fasciculated and many did not enter the OD. (F) Same image as E with the green channel (axons) removed. The density of nuclei was not reduced when compared with that of the wild type. (G) Low magnification of a *Brn3b/Brn3c* double mutant retina labeled with the same antibodies as in A. Axons were barely detectable (arrows). (H) An enlarged view from the highlighted area shown in G. The axon number was further reduced when compared with E, but misrouted axons were not observed. The thick green-labeled tubule structures were capillaries that label non-specifically. (I) Same image as that in H with green channel removed. A slightly reduced nuclei number was detected in the vacant areas, but the reduction was not significant when compared with *Brn3b*$^{-/-}$ retinas.

retina when compared with a wild-type control (Fig. 5J,K), and was virtually absent in the *Brn3b/Brn3c* double mutant retina (Fig. 5L).

Closer examination of the ganglion cell layer revealed an average of 15±3 RGCs (n=6) over a distance of 200 μm in wild-type retina (Fig. 5M; white arrows point to RGCs), with about a third of the ganglion cell layer composed of displaced amacrine cells (Fig. 5M). In *Brn3b*$^{-/-}$ retinas, 6±2 RGCs (n=6) were identified over the same distance, and displaced amacrine cells occupied two-thirds of the population in the ganglion cell layer (Fig. 5N). In the double-mutant retinas, the RGC number was reduced to 2±2 (n=6), and although the number of amacrine cells was not substantially increased from that found in *Brn3b*$^{-/-}$ retinas, almost 90% of the cells in the ganglion layer were displaced amacrine cells (Fig. 5O). These results further demonstrate that Brn3c has a compensatory function in RGC differentiation and axon formation that is uncovered in *Brn3b/Brn3c* double knockout mice. Mice that are deficient in *Math5* (*Atoh7* – Mouse Genome Informatics) or *Pax6* genes are unable to specify RGCs, and in retinas of *Math5*$^{-/-}$ and *Pax6*$^{-/-}$ mice, missing RGCs are also replaced by amacrine cells, probably because of a respecification of RGC progenitors (Wang et al., 2001; Marquardt et al., 2001).

Axon pathfinding defects in *Brn3b*$^{-/-}$ and *Brn3b/Brn3c* double mutant mice.

Brn3b/Brn3c double mutant retinas but not *Brn3b*$^{-/-}$ retinas, suffered from a greater loss of projections emanating from the ventral-temporal region than from the dorsal-nasal region (Fig. 5C,F). In the adult mouse, ipsilateral projections are restricted to RGCs within the ventral-temporal crescent of the retina (Dräger, 1985). It was therefore possible that Brn3c was associated with controlling the ipsilateral growth of RGC axons, and in *Brn3b/Brn3c* double mutant adult retinas, a defect in ipsilateral projections would be apparent. To test this possibility, we performed anterograde labeling of RGCs with P2 wild-type, *Brn3b*$^{-/-}$ and *Brn3b-brn3c* double mutant mice.

Right-side retinas were labeled with DiI (Fig. 7, red), and left-side with DiASP (Fig. 7, green). Optic chiasms were examined 20-24 hour after dye injection. In wild-type optic chiasms, the majority of axons projected contralaterally, but a small proportion of ipsilateral axons was clearly seen (Fig. 7A,D). In *Brn3b*$^{-/-}$ optic chiasms, the total number of axons was reduced, indicating that the majority of RGC axons were not able to reach the optic chiasm (Fig. 7B,E). Many of the axons that reached the optic chiasm of *Brn3b*$^{-/-}$ mice were abnormal. They were misrouted dorsally toward the hypothalamus (12/12 examples) or occasionally went into the optic nerve of the other eye (4/12 examples) (Fig. 7B,E). Misrouting of RGC axons in *Brn3b*$^{-/-}$ mice has been reported previously by Erkman et al. (Erkman et al., 2000). Interestingly, a larger proportion of axons was directed ipsilaterally in *Brn3b*$^{-/-}$ mice, making the ipsilateral/contralateral ratio almost 1.0 (Fig. 7E).

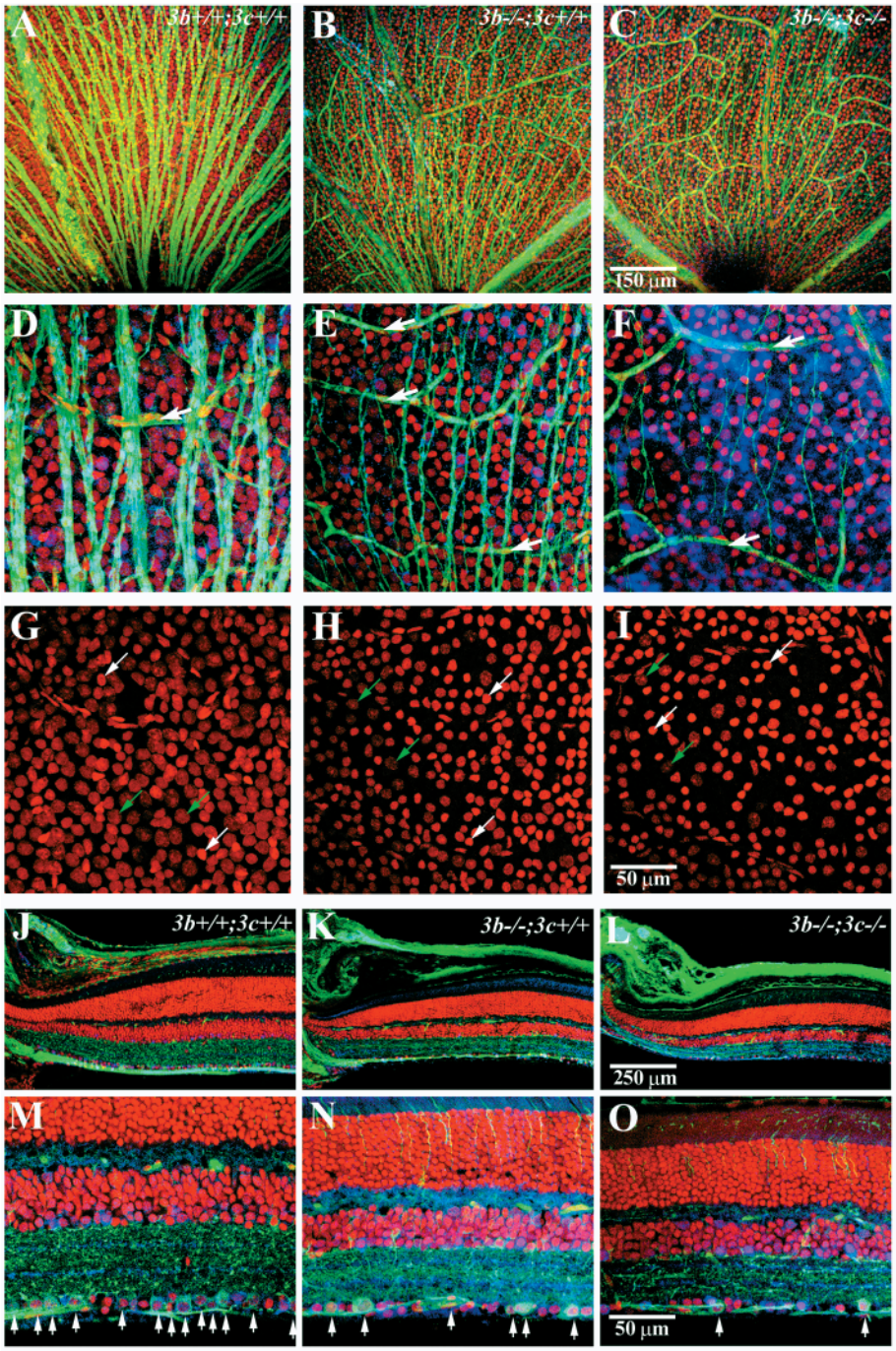

Fig. 5. RGC and axon distribution in 3-week-old retinas. (A-C) Wild-type (A), *Brn3b*$^{-/-}$ (B) and *Brn3b/Brn3c* double mutant (C) retinas from the dorsal-nasal region. Retinas were labeled with anti-β3-tubulin (RGCs and axons, green) and propidium iodide (nuclei, red). The number of axons in the *Brn3b*$^{-/-}$ retina (B) was greatly reduced when compared with that of the wild type (A). The number of axons deceased only slightly in the double-mutant retina (C). The thick branching green-labeled structures are blood vessels and capillaries nonspecifically labeled. (D-F) Enlarged views of wild-type (D), *Brn3b*$^{-/-}$ (E) and *Brn3b/Brn3c* double-mutant (F) retinas from the ventral-temporal region. Optic disks are located at the bottom out of frame. Retinas were labeled with anti-β3-tubulin (RGCs and axons, green), ChAT (displaced amacrine cells, blue) and propidium iodide (nuclei, red). The number of axons was greatly reduced in the *Brn3b/Brn3c* double mutant retina (F) when compared with a *Brn3b*$^{-/-}$ retina (E). The thick branching green-labeled structures (arrows) are blood vessels and capillaries that were nonspecifically labeled with anti-mouse IgG secondary antibody. Note that excess capillaries were embedded in the RGC layer. Some large nuclei are surrounded by ChAT-positive signals in F. It is possible that these signals resulted from the processes of the overproduced amacrine cells. (G-I) The same images as D-F with the green and blue channels removed. The smaller condensed nuclei (blue arrows) correspond to ChAT-positive amacrine cells, while the large diffuse nuclei (green arrows) correspond to RGCs. (J-L) Low-magnification views of cross sections collected from wild-type (J), *Brn3b*$^{-/-}$ (K) and *Brn3b/Brn3c* double mutant (L) retinas. Sections were labeled as in D-F. Note the optic fiber layer in green at the bottom of the *Brn3b*$^{-/-}$ retina (K) is much thinner than that of the wild-type retina (J), and the optic fiber in the double mutant retina (L) is barely detectable. (M-O) Enlarged views of cross sections collected from wild-type (M), *Brn3b*$^{-/-}$ (N) and *Brn3b/Brn3c* double mutant (O) retinas. Labeling was the same as in D-F. RGCs are indicated by arrowheads.

In optic chiasms of *Brn3b/Brn3c* double knockout mice, the axon number was further reduced (Fig. 7C,F). Unexpectedly, the misrouted axons observed in *Brn3b*$^{-/-}$ optic chiasms were not found in the double mutants (Fig. 7C,F; n=6). In addition, virtually no ipsilateral projections were seen in the double mutant optic chiasms (Fig. 7F). The results suggest that in the absence of Brn3b and Brn3c, RGC axons defaulted to a contralateral pathway, presumably because RGCs from the ventral-temporal region of the retina were missing. Brn3c appears to promote enhanced ipsilateral growth and axon misrouting in *Brn3b*$^{-/-}$ mice, as both of these defects were eliminated in the double mutant.

Viral vector-mediated expression of *Brn3c* promotes neurite formation in the absence of Brn3b

We next asked whether Brn3c was sufficient for promoting axon growth in RGCs that were deficient in this process. Cultured retinal explants from E13.5 *Brn3b*$^{-/-}$ embryos extend abnormal processes that are short, tangled and dendritic in character (Fig. 3E) (Wang et al., 2000). Except for neurite and migration defects, *Brn3b*$^{-/-}$ RGCs appeared to be well differentiated and should therefore be useful in attempts to restore axon outgrowth. When *Brn3b* was expressed in *Brn3b*$^{-/-}$ retinal explants by HSV-mediated gene transfer (Bowers et al., 2001), effective restoration of axon outgrowth

was observed (data not shown). We repeated the experiment using an HSV amplicon containing *Brn3c* (Fig. 8A). In this amplicon, a *GFP* sequence was expressed under separate control (Fig. 8A). Fig. 8B,C shows efficient *GFP* expression in an explant derived from a *Brn3b*$^{-/-}$ retina infected with an HSV amplicon lacking *Brn3c*. Expression was found in most cells within the explanted tissue (Fig. 8B) and in neurites extending outward from the tissue (Fig. 8C). These neurites were the dendrite-like processes reported previously (Wang et al., 2000). Moreover, abnormal migrating RGCs characteristic of *Brn3b*-deficient retinas were present at the edge of the tissue (Fig. 8C). When *Brn3c* was included in the amplicon, *GFP* expression was similar to the control vector (Fig. 8D). The abnormally migrating RGCs were not observed and the number of neurites extending outward increased tenfold (Fig. 8E). In addition, the neurites were substantially longer in *Brn3b*$^{-/-}$ explants that expressed *Brn3c* (Fig. 8E). However, the neurites did not resemble normal axons in that they were highly branched (Fig. 8E, inset) suggesting that Brn3b and Brn3c did not function identically to each other in this gain-of-function analysis.

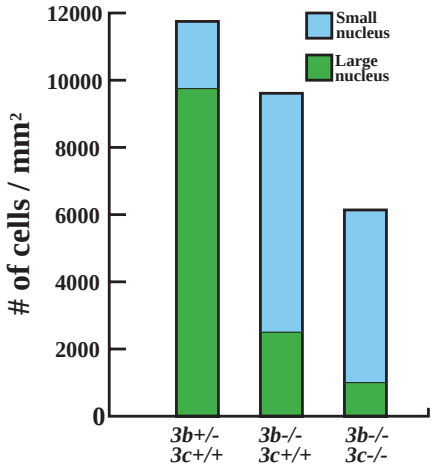

Fig. 6. Altered cell population in the ganglion cell layer of *Brn3b*$^{-/-}$ and *Brn3b/Brn3c* double mutant retinas. Six 200 × 200 μm images collected from three different retinas from each indicated genotype were scored for small (amacrine, blue) and large (RGC, green) nuclei. Ambiguous nuclei were counted and assigned equally to each category.

DISCUSSION

Compensatory functions for Brn3b and Brn3c in RGC differentiation

In this study, we have shown that *Brn3c* has critical functions in RGC axon outgrowth. These functions were not apparent in mice with a targeted deletion solely at the *Brn3c* locus but were revealed in *Brn3b/Brn3c* double knockout mice. *Brn3c* is expressed in approximately 50% of RGCs, while *Brn3b* is expressed in virtually all RGCs (Xiang et al., 1995; Gan et al., 1999; Wang et al., 2000). The subpopulation of *Brn3b/Brn3c*-

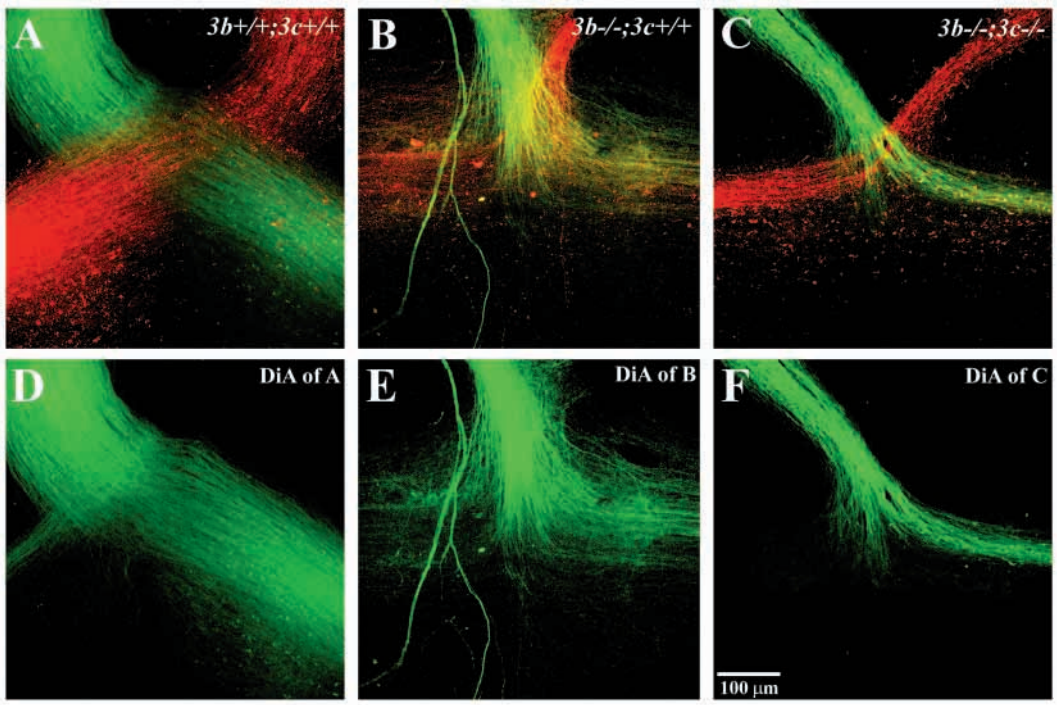

Fig. 7. Anterograde-labeled optic chiasms from wild-type, *Brn3b*$^{-/-}$ and *Brn3b/Brn3c*-double mutant mice. At P2, DiI (red) was injected into the vitreous space of right eyes and DiASP (green) into left eyes. Images were collected with a confocal microscope at P3 through the visible thickness of the optic chiasms at 5 μm intervals. (A) Wild-type optic chiasm showing representative decussation. (B) *Brn3b*$^{-/-}$ optic chiasm showing highly abnormal crossing patterns. Optic nerves were thinner than those from wild-type and many axons were observed sprouting from the optic nerve and projecting to the ventral hypothalamus. (C) *Brn3b/Brn3c* double-mutant optic chiasm showing partially restored decussation. (D-F) Axons from the left eye of those shown in A-C to visualize the small portion of ipsilaterally projecting axons. Note the abnormally abundant ipsilateral axons in E and the absence of misrouted and ipsilateral axons in F.

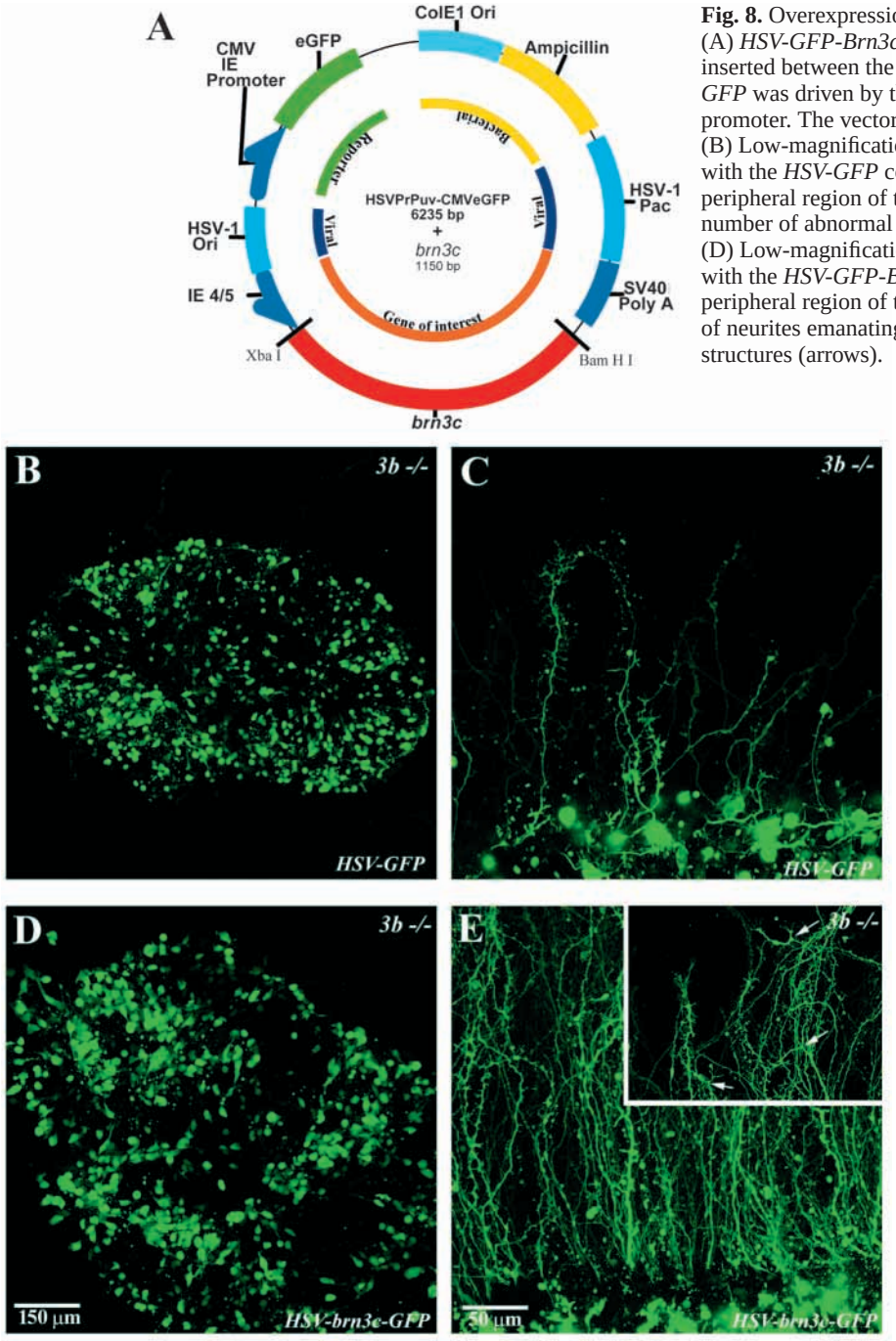

Fig. 8. Overexpression of *HSV-GFPBrn3c* in retinal explants. (A) *HSV-GFP-Brn3c* amplicon. The coding region of *Brn3c* was inserted between the *Xba*I and *Bam*HI sites of the amplicon vector. *GFP* was driven by the CMV promoter, and *Brn3c* by the HSV IE4/5 promoter. The vector without the *Brn3b* insert served as a control. (B) Low-magnification view of a *Brn3b*$^{-/-}$ retinal explant infected with the *HSV-GFP* control amplicon. (C) An enlarged view of the peripheral region of the same sample as in B, showing a small number of abnormal neurites emanating from the tissue body. (D) Low-magnification view of a *Brn3b*$^{-/-}$ retinal explant infected with the *HSV-GFP-Brn3c* amplicon. (E) An enlarged view of the peripheral region of the same sample as in D showing a large number of neurites emanating from the tissue body. Inset shows branched structures (arrows).

expressing RGCs represents the cells that are probably affected in the double mutants.

When Brn3c, but not Brn3b, was absent from cells normally expressing both *Brn3b/Brn3c*, RGC differentiation and axon formation occurred. When Brn3b, but not Brn3c, was missing, the cells sent out abnormal processes. When both Brn3b and Brn3c were missing, cells normally expressing both *Brn3b* and *Brn3c* were present, which indicated that the RGC differentiation program had occurred, but the RGCs were unable to extend even abnormal axons. The absence of Brn3b and Brn3c led to a loss of *Brn3b/Brn3c*-expressing RGCs in adults. Presumably, these cells underwent apoptosis because they could not extend axons. RGCs in the ventral-temporal region of the adult retina were more severely affected by the loss of Brn3b and Brn3c than were cells in the dorsal-nasal region, implying that the ventral-temporal region in wild-type mice is enriched in *Brn3b/Brn3c*-expressing cells. Indeed, ipsilateral projections are missing at the optic chiasm of *Brn3b/Brn3c* double knockouts, suggesting that Brn3c may be involved in the control of ipsilateral guidance.

The distinct phenotypes exhibited by *Brn3a*$^{-/-}$, *Brn3b*$^{-/-}$ and *Brn3c*$^{-/-}$ mice had previously suggested a simple model in which each Brn3 factor was necessary for the terminal differentiation and survival of an individual sensory system (Xiang et al., 1997b). Of particular relevance, Brn3b was shown to be required for the normal differentiation of RGCs (Erkman et al., 1996; Gan et al., 1996) and Brn3c for auditory and vestibular hair cells (Erkman et al., 1996; Xiang et al., 1997a). The work described here demonstrates that a more complex relationship must exist between Brn3b and Brn3c in the regulation of RGC gene expression. The absence of both *Brn3b* and *Brn3c* genes resulted in a more severe RGC defect than that observed for either single deletion. In fact, published studies on mice that lack only *Brn3c* have yet to reveal any RGC defects, indicating that the role of Brn3c role in RGC differentiation can be largely or entirely replaced by other factors, most likely Brn3a and Brn3b. Conversely, the RGC phenotype of *Brn3b/Brn3c* double mutant mice demonstrates that Brn3c plays a compensatory role in the absence of Brn3b. Thus, Brn3b and Brn3c appear to have partially overlapping roles in RGC axon outgrowth, despite the fact that *Brn3b* is expressed much earlier in development than *Brn3c*.

Roles for Brn3b and Brn3c in promoting axon outgrowth

We made use of a gain-of-function analysis using *Brn3b*$^{-/-}$

retinal explants to demonstrate that Brn3c was able to promote axon outgrowth, even in the absence of Brn3b. The results indicate that high levels of Brn3c suffice to perform many of the functions normally required by both Brn3b and Brn3c. However, the axons in *Brn3c*-expressing cells were not normal, and it is therefore possible that Brn3c cannot replace all the functions of Brn3b. We favor the notion that Brn3b and Brn3c have distinct as well as overlapping functions in promoting axon outgrowth in differentiating RGCs. These functions must ultimately relate to the sets of genes that are dependent on Brn3b, Brn3c, or both factors for their expression.

The *Brn3b*$^{-/-}$ retinal explants contained other cell types besides RGCs, and our analysis did not distinguish whether HSV-mediated expression of *Brn3c* (or *Brn3b*) could promote axon outgrowth in non-RGCs or whether the outgrowth was limited to RGCs. This is an interesting distinction because *Brn3b*$^{-/-}$ RGCs are at least partially differentiated, whereas non-RGCs within the *Brn3b*$^{-/-}$ explants are likely to include uncommitted neuroblasts and neuroblasts that are committed to non-RGC fates. Axons emanating from these cells as a result of *Brn3c* misexpression would suggest a much broader function for Brn3c. Thus, Brn3c might be capable of initiating the RGC differentiation program in non-RGCs of explanted retina. Consistent with this notion, Liu et al. (Liu et al., 2000) showed that all three Brn3 genes can promote RGC fate in non-RGC progenitors in the chick retina.

Roles for Brn3b and Brn3c in axon pathfinding

A recent study showed that Brn3b regulated genes associated with axon pathfinding in adult mice (Erkman et al., 2000). The residual axons emanating from *Brn3b*$^{-/-}$ RGCs exhibit pathfinding defects at every point where axons make decisions about which way to project. Pathfinding defects were found at the peripheral retina, optic disk, optic nerve, optic chiasm and superior colliculus (Erkman et al., 2000). In addition, residual *Brn3b*$^{-/-}$ axons do not fasciculate in early retinogenesis. Several genes involved in axon outgrowth and pathfinding have recently been identified as potential target genes of Brn3b by differential hybridization screens, including those for neuritin and Gap43 (Erkman et al., 2000; Mu et al., 2001).

Defects in *Brn3b*$^{-/-}$ residual axons are particularly noticeable at the optic chiasm. In addition to misrouted axons, the number of axons projecting ipsilaterally is substantially increased in *Brn3b*$^{-/-}$ mice. There may be a close relationship between misguided axons and ipsilateral axons. In normal axon guidance, RGC axons that eventually project ipsilaterally do so by trial and error, and during development many axon projections appear to be wandering; the projections that do not migrate ipsilaterally eventually undergo apoptosis (Godement et al., 1994; Marcus and Mason, 1995).

In contrast to *Brn3b*$^{-/-}$ optic chiasms, those from *Brn3b/Brn3c* double mutants had virtually no misrouted or ipsilateral RGC axons. These results indicate that the presence of Brn3c and the absence of Brn3b enhanced the production of ipsilateral projections, while the absence of Brn3c and Brn3b enhanced their loss. The most severe loss of RGCs in *Brn3b/Brn3c* double knockout mice derives from the ventral-temporal region of the adult retina, where ipsilateral projections originate. Thus, Brn3c appeared to be required for ipsilateral projections in the subpopulation of *Brn3b/Brn3c*-expressing cells in the ventral-temporal region of the retina. Preliminary evidence indicates that ipsilateral projections are also missing at the optic chiasm of *Brn3c*$^{-/-}$ mice (S. W. W., unpublished). This suggests that Brn3c has a specialized function in axon pathfinding that cannot be replaced by Brn3b or other factors.

During RGC axonogenesis, each Brn3 factor regulates distinct as well as overlapping sets of genes required for the formation of the final RGC axonal network. Although *Brn3a*$^{-/-}$ mice display no observable retinal phenotype, we predict that roles for Brn3a in RGC differentiation will be uncovered in *Brn3a/Brn3b* and *Brn3a/Brn3c* double knockout mice, and in *Brn3a/Brn3b/Brn3c* triple knockout mice. Moreover, it is likely that the distinct and overlapping requirements for the Brn3 factors in axonogenesis will extend to dorsal root and trigeminal ganglia, the other projection neurons expressing the Brn3 genes.

We thank Darlene Howard and Ann Casey for assistance in packaging HSV amplicons. Genotype analysis was performed by Lin Liu. We acknowledge the National Eye Institute (EY11930) and the Robert A. Welch foundation for their support to W. H. K. The HSV amplicon project is supported by an AFAR Grant to W. J. B. and an National Institute of Aging grant (AG18254) to H. J.F.

REFERENCES

Bowers, W. J., Howard, D. F. and Federoff, H. J. (2000). Discordance between expression and genome transfer titering of HSV amplicon vectors: recommendation for standardized enumeration. *Mol. Ther.* **1**, 294-299.

Bowers, W. J., Howard, D. F., Brooks, A. I., Halterman, M. W. and Federoff, H. J. (2001). Expression of vhs and VP16 during HSV-1 helper virus-free amplicon packaging enhances titers. *Gene Ther.* **8**, 111-120.

Dräger, U. (1985). Birth dates of retinal ganglion cells giving rise to the crossed and uncrossed optic projections in the mouse. *Proc. R. Soc. London* **224**, 57-77.

Duggan, A., Ma, C. and Chalfie, M. (1998). Regulation of touch receptor differentiation by the Caenorhabditis elegans mec-3 and unc-86 genes. *Development* **125**, 4107-4119.

Eng, S. R., Gratwick, K., Rhee, J. M., Fedtsova, N., Gan, L. and Turner, E. E. (2001). Defects in sensory axon growth precede neuronal death in Brn3a-deficient mice. *J. Neurosci.* **21**, 541-549.

Erkman, L., McEvilly, R. J., Luo, L., Ryan, A. K., Hooshmand, F., O'Connell, S. M., Keithley, E. M., Rapaport, D. H., Ryan, A. F. and Rosenfeld, M. G. (1996). Role of transcription factors Brn-3.1 and Brn-3.2 in auditory and visual system development. *Nature* **381**, 603-606.

Erkman, L., Yates, P. A., McLaughlin, T., McEvilly, R. J., Whisenhunt, T., O'Connell, S. M., Krones, A. I., Kirby, M. A., Rapaport, D. H., Bermingham, J. R. et al. (2000). A POU domain transcription factor-dependent program regulates axon pathfinding in the vertebrate visual system. *Neuron* **28**, 779-792.

Fields-Berry, S. C., Halliday, A. L. and Cepko, C. L. (1992). A recombinant retrovirus encoding alkaline phosphatase confirms clonal boundary assignment in lineage analysis of murine retina. *Proc. Natl. Acad. Sci. USA* **89**, 693-697.

Gan, L., Xiang, M., Zhou, L., Wagner, D. S., Klein, W. H. and Nathans, J. (1996). POU domain factor Brn-3b is required for the development of a large set of retinal ganglion cells. *Proc. Natl. Acad. Sci. USA* **93**, 3920-3925.

Gan, L., Wang, S. W., Huang, Z. and Klein, W. H. (1999). POU domain factor Brn-3b is essential for retinal ganglion cell differentiation and survival but not for initial cell fate specification. *Dev. Biol.* **210**, 469-480.

Godement, P., Wang, L. C. and Mason, C. A. (1994). Retinal axon divergence in the optic chiasm: dynamics of growth cone behavior at the midline. *J. Neurosci.* **14**, 7024-7039.

Goldberg, J. L. and Barres, B. A. (2000). The relationship between neuronal survival and regeneration. *Annu. Rev. Neurosci.* **23**, 579-612.

Huang, E. J., Zhang, K., Schmidt, A., Saulys, A., Xiang, M. and Reichardt,

L. F. (1999). POU domain factor Brn-3a controls the differentiation and survival of trigeminal neurons by regulating Trk receptor expression. *Development* **126**, 2869-2882.

Liu, W., Khare, S. L., Liang, X., Peters, M. A., Liu, X., Cepko, C. L. and Xiang, M. (2000). All Brn3 genes can promote retinal ganglion cell differentiation in the chick. *Development* **127**, 3237-3247.

Marcus, R. C. and Mason, C. A. (1995). The first retinal axon growth in the mouse optic chiasm: axon patterning and the cellular environment. *J. Neurosci.* **15**, 6389-6402.

Marquardt, T., Ashery-Padan, R., Andrejewski, N., Scardigli, R., Guillemot, F. and Gruss, P. (2001). Pax6 is required for the multipotent state of retinal progenitor cells. *Cell* **105**, 43-55.

McEvilly, R. J., Erkman, L., Luo, L., Sawchenko, P. E., Ryan, A. F. and Rosenfeld, M. G. (1996). Requirement for Brn-3.0 in differentiation and survival of sensory motor neurons. *Nature* **384**, 574-577.

Mu, X., Zhao, S., Pershad, R., Hsieh, T.-F., Scarpa, A., Wang, S. W., White, R. A., Beremand, P. D., Thomas, T. L., Gan, L. and Klein, W. H. (2001). Gene expression in the developing mouse retina by EST sequencing and microarray analysis. *Nucleic Acids Res.* (in press).

Rohrig, S., Rockelein, J., Donhauser, R. and Baumeister, R. (2000). Protein interaction surface of the POU transcription factor UNC-86 selectively used in touch neurons. *EMBO J.* **19**, 3694-3703.

Sze, J. Y., Liu, Y. and Ruvkun, G. (1997). VP16-activation of the *C. elegans* neural specification transcription factor UNC-86 suppresses mutations in downstream genes and causes defects in neural migration and axon outgrowth. *Development* **124**, 1159-1168.

Wang, S. W., Gan, L., Martin, S. E. and Klein, W. H. (2000). Abnormal polarization and axon outgrowth in retinal ganglion cells lacking the POU-domain transcription factor brn-3b. *Mol. Cell. Neurosci.* **16**, 141-156.

Wang, S. W., Kim, B.-S., Ding, K., Wang, H., Sun, D., Johnson, R. L. and Klein, W. H. (2001). Requirement for math5 in the development of retinal ganglion cells. *Genes Dev.* **15**, 24-29.

Xiang, M. (1998). Requirement for Brn-3b in early differentiation of postmitotic retinal ganglion cell progenitors. *Dev. Biol.* **197**, 155-169.

Xiang, M., Zhou, L., Macke, J. P., Yoshioka, T., Hendry, S. H., Eddy, R. L., Shows, T. B. and Nathans, J. (1995). The Brn-3 family of POU-domain factors: primary structure, binding specificity, and expression in subsets of retinal ganglion cells and somatosensory neurons. *J. Neurosci.* **15**, 4762-4785.

Xiang, M., Gan, L., Zhou, L., Klein, W. H. and Nathans, J. (1996a). Targeted deletion of the mouse POU domain gene Brn-3a causes selective loss of neurons in the brainstem and trigeminal ganglion, uncoordinated limb movement, and impaired suckling. *Proc. Natl. Acad. Sci. USA* **93**, 11950-11955.

Xiang, M., Zhou, H. and Nathans, J. (1996b). Molecular biology of retinal ganglion cells. *Proc. Natl. Acad. Sci. USA* **93**, 596-601.

Xiang, M., Gan, L., Li, D., Chen, Z.-Y., Zhou, L., O'Malley, B. W., Jr, Klein, W. and Nathans, J. (1997a). Essential role of POU-domain factor Brn-3c in auditory and vestibular hair cell development. *Proc. Natl. Acad. Sci. USA* **94**, 9445-9450.

Xiang, M., Gan, L., Li, D., Zhou, L., Chen, Z. Y., Wagner, D. S., O'Malley, B. W., Jr, Klein, W. and Nathans, J. (1997b). Role of Brn-3 family of POU-domain genes in the development of auditory/vestibular, somatosensory, and visual systems. *Cold Spring Harb. Symp. Quant. Biol.* **62**, 325-336.

Xiang, M., Gao, W. Q., Hasson, T. and Shin, J. J. (1998). Requirement for Brn-3c in maturation and survival, but not in fate determination of inner ear hair cells. *Development* **125**, 3935-3946.